Earthquakes and Structures, Vol. 3, No. 3-4 (2012) 365-381 365
DOI: http://dx.doi.org/10.12989/eas.2012.3.3.365

Influence of some relevant parameters in the seismic vulnerability of RC bridges

B.A. Olmos*, J.M. Jara and M. Jara

Facultad de Ingeniería Civil, Universidad Michoacana de San Nicolás de Hidalgo, México

(Received June 19, 2011, Revised January 17, 2012, Accepted April 10, 2012)

Abstract. Recent earthquakes have damaged some bridges located on the Pacific Coast of Mexico; these bridges have been retrofitted or rebuilt. Based on the fact that the Pacific Coast is a highly active seismic zone where most of the strong earthquakes in the country occur, one fertile and important area of research is the study of the vulnerability of both new and existent bridges located in this area that can be subjected to strong earthquakes. This work is focused on estimating the contribution of some parameters identified to have major influence on the seismic vulnerability of reinforced concrete bridges. Ten models of typical reinforced concrete (RC) bridges, and two existing bridges located close to the Pacific Coast of Mexico are considered. The group of structures selected for the study is based on two span bridges, two pier heights and two substructure types. The bridges were designed according to recent codes in Mexico. For the vulnerability study, the capacity of the structure was evaluated based on the FEMA recommendations. On the other hand, the demand was evaluated using a group of more than one hundred accelerograms recorded close to the subduction zone of Mexico. The results show that the two existent bridges analyzed show similar trends of behavior of the group of bridge models studied. In spite of the contribution that traditional variables (height and substructure type) had to the bridge seismic response, the bridge length was also found to be one of the parameters that most contributed to the seismic vulnerability of these RC medium-length bridges.

Keywords: bridges; fragility curves; bridge vulnerability; RC bridges; medium-length bridges' vulnerability

1. Introduction

Advances in technology and knowledge have allowed more rational improvements on the well-known design codes. The general trend is towards performance-based design based on probabilistic models that lately has caught researchers' attention. In this vein, there are several studies directed toward reinforced concrete and steel bridges, and many of the results and conclusions achieved in those works have already been incorporated based on codes such as FEMA-273 and ATC-40. This is a fertile area for future research since many of the existent bridges were built a long time ago for different live and accidental loads than those currently proposed on the regulation codes. Keeping in mind the fact that the design of existent bridges has been carried out using conservative safety factors, and during the design process each of the parts that conform a bridge have been designed considering a single component rather than the contribution of the whole system, the real resistance

*Corresponding author, Ph.D., E-mail: bolmos@umich.mx

of the bridge might be greater than the capacity of loading evaluated during the design processes. This fact can be one of the reasons for not having dramatic damage on the highway bridges due to the increments on the live load amplitudes. So, it would be very convenient to develop system reliability models that include the most significant random variables for the evaluation of the reliability and vulnerability of the bridges located in a specific region.

The Mexican highway system has been in expansion during recent decades. Its development requires the construction of new bridges or the rehabilitation of the existing ones. Mexico is affected by several seismic faults (subduction, normal, transformation and deeper inslab earthquakes). Most of the strong earthquakes have epicenters in a zone of the Pacific Coast situated at the boundaries of the Pacific and North-American Plates. Many of the bridges were built in areas considered with moderate or high seismicity according to the seismic zonation of the country, making this an additional issue to be considered for estimating the vulnerability of bridges located in this area. The vulnerability assessment of existing bridges is of great importance given the fact that most of them were designed according to design projects developed more than 40 years ago. This produces an important group of bridges that are particularly vulnerable to earthquake occurrence. Moreover, new bridges are continuously built in these zones making it important to reevaluate the seismic vulnerability of these structures.

Fragility curves are a valuable tool to assess different damage levels as a function of possible seismic scenarios. These curves relate the probability of reaching a certain damage state of a specific structure or of a group of structures with ground motion intensities. Moses (1999) presented bridge reliability concepts and methods that can be used as antecedents of the bases of this subject. There are some studies considering just a few random variables in demand and capacity and others using probability density functions to describe most of the variables involved. Some of the methodologies proposed in the literature to assess the seismic vulnerability of structures are described by Hwang *et al*. 1998, 2000, Gomez *et al*. 2002, Banerjee and Shinozuka 2007, Dutta and Mander 1998, Kasperski *et al*. 2006, Mackie and Stojadinovic 2006, Nielson 2005, Karim and Yamazaki 2003, Yi *et al*. 2009 and Pagnini *et al*. (2011). Some of these methods have also been proposed to evaluate the expected behavior of retrofitted bridges or bridge elements (Padgett 2005, Fridley and Ma 2007, Kim and Shinozuka 2004).

There are in the literature several approaches to estimate capacity and demand. Some criteria were developed with the aim of being easy to handle for practitioner engineers (Gómez *et al*. 2002). Typically, the bridge capacity was assessed using nonlinear static methods or nonlinear dynamic analyses. When incremental non-linear static procedure was performed, the load pattern was mostly selected according to the mode shapes of the bridge. On the other hand, nonlinear dynamic approaches use step-by-step numerical solutions for assessing the capacity with the consuming computer time inconvenience. In this methodology, it is relevant to appropriate assess the dynamic characteristics of the bridges; several studies related with this topic has been published (Ali 2011). The demand was usually estimated based on a group of selected accelerograms recorded from real earthquakes or by a group of synthetic records (Panza *et al*. 2001). There are other studies (DiPasquale and Cakmak 1990) that proposed damage indexes to estimate the seismic vulnerability. Other researchers proposed fragility curves to quantify the bridges' probability of exceedance for different limit states of the structural seismic behavior accounting for selected variables, (Peckcan 1998, Dutta and Mander 1998). Shinozuka *et al*. (2007) and Jara *et al*. (2011), have compared fragility curves constructed with nonlinear static analysis with the fragility curves developed with time-history dynamic analysis, and they found well consistency that proves the reliability of the nonlinear static procedure. In some other cases, the authors use response spectra to quantify the uncertainty of the demand parameters (Moustafa 2011).

In all the proposals, the main objective was to get results that allow the estimation of the expected bridge response for different seismic scenarios. In Mexico, an important number of works to estimate the seismic vulnerability of structures located in urban areas, using not only simplified but also complex methodologies have been developed. In spite of that, little effort has been made to study the actual seismic vulnerability of new and existent bridges.

2. Bridge models

The analytical models for the bridges considered in this study correspond to 2-typical span RC bridges built in Mexico, with span lengths of 20 and 40 m, pier heights of 6 and 10 m, and two types of piers; a single column and a three-column bent integrally connected at the top to a rigid cross bent cap beam forming a frame type substructure in transverse direction. The bridges are located in the Pacific Coast region of Mexico, the area of the highest seismic hazard in Mexico. The 3D structural models were analyzed with the aid of the SAP2000 program. The superstructure of the bridges has an 18 cm depth slab supported on longitudinal prestressed AASHTO type beams, RC diaphragms located at the ends and every 10 m between the support axes, RC bent caps located at each support line and circular RC columns. The girders, diaphragms, bent caps and piers were modeled as beam elements, but the RC slab was modeled with a mesh of rectangular thin shell (plate bending and stretching) finite elements. The beams were supported on neoprene-laminated bearings that were represented with linear link elements. The abutments were not included in the model neglecting the flexibility of their foundations and the pier supports were considered fixed (Fig. 1). For design, live loads trucks currently used in Mexico were considered, *HS*-20, *T*3-*S*3 and *T*3-*S*2-*R*4 with total weight of 321.8, 451.3 and 761.63 kN, respectively. An importance factor of 1.5 was used as it is stipulated in codes for structures classified in the group A (important structures). Three load combinations were considered for the design as stipulated in the AASHTO code, the first to combine the dead and live loads, the second for the dead plus earthquake acting in the longitudinal direction, and the third was for dead plus earthquake acting on the transverse direction. The seismic design loads were evaluated using a response spectrum analyses with the complete quadratic combination (CQC) rule. Twenty modes of vibration were considered, assuming

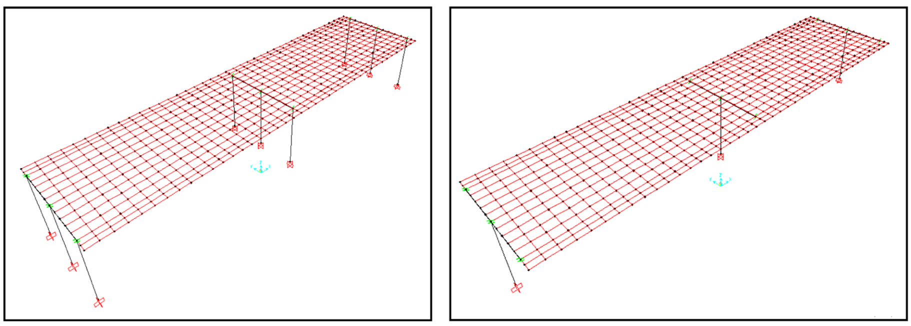

(a) (b)

Fig. 1 Structural bridge model for substructures formed by (a) three piers and (b) one pier a constant damping value of 5%.

In addition to the bridges previously described, we studied two existent bridges located in the highest seismic zone of the country, the Chuta (one column substructure) and the Feliciano bridges (two-column frame type substructure). The Chuta Bridge (Fig. 2) is located on the highway Playa

Fig. 2 Longitudinal view of La Chuta Bridge

Fig. 3 Transverse and longitudinal view of Feliciano Bridge

Azul-Manzanillo in the State of Michoacan in Mexico. The bridge superstructure is a continuous prestressed concrete box, 9.90 m wide and 1.80 m high, resting on rubber laminated bearings supported by the piers' bent cap. It has five spans of approximately 35 m each, and two end spans of 29.60 m given a total length bridge of 233.60 m. The substructure is formed by six single column piers with circular transverse section of 2 m diameter. The piers' heights vary from 5.30 m at the end spans of the bridge to 8.60 m at the central spans of the bridge. The cap beam is a variable cross section with a width of 1.45 m and the maximum depth is 1.65 m.

The Feliciano Bridge (Fig. 3) is located on the highway Lázaro Cárdenas-Uruapan in the State of Michoacan in Mexico. The bridge has four simple supported spans with lengths in the range of 29 m to 34 m. The superstructure was built by an RC slab resting on ten prestressed AASHTO-type beams, and they are simple supported over laminated rubber bearings. The substructure is a frame type pier built with two square RC columns of 1.95 m width and 14 m height connected to a rectangular RC bent cap.

3. Seismic hazard assessment

A seismic hazard assessment for the sites where the bridges are located was carried out, aimed at determining the expected peak ground acceleration for different return periods. All the seismic faults that contribute to the seismic hazard of the Pacific Coast region in Mexico were considered in the analysis. Specific attenuation laws obtained for subduction and intraplate Mexican sources were used (Garcia *et al*. 2005, Sanchez and Jara 2001) and a more general law for local type sources (Abrahamson and Silva 1997). The earthquake occurrence process was divided into two models namely: (a) characteristic process associated with subduction earthquakes with magnitude equal to or greater than 7.0, which present evident occurrence periodicity and magnitude dependence on the elapsed time between their occurrences as well and (b) poisson model for other faults and subduction events with magnitude less than 7.0. The maximum expected magnitudes for the characteristic process were adopted from Rosenblueth and Ordaz (1989). An empirical equation of the expected magnitude (M) of the characteristic earthquakes as a function of the occurrence elapsed time (t) was determined (Eq. (1)).

$$E[M|t] = max(7.5, 4.71 + 0.757 \ln t) \tag{1}$$

A lognormal distribution for the time between characteristic earthquakes $f_T(t)$, was selected (Jara and Rosenblueth 1988)

$$f_T(t|t_0) = \frac{1}{kt\sqrt{2\pi}\sigma_{\ln t}} e^{-\frac{1}{2\sigma_{\ln t}^2}(\ln t - \ln m_t)^2} \tag{2}$$

where

$$k = \int_{t_0}^{\infty} \frac{1}{t\sqrt{2\pi}\sigma_{\ln t}} e^{-\frac{1}{2\sigma_{\ln t}^2}(\ln t - \ln m_t)^2} \tag{3}$$

and the parameters of the distribution are $m_t = 40.6$ years and $\sigma_{\ln t} = 0.39$ according to seismicity data

Table 1 Expected PGA at the Pacific Coast in Mexico

Return period (years)	50	235	500	1000
PGA (gals)	255	480	645	820

of the subduction sources in Mexico. t_0 is the elapsed time since the last characteristic earthquake for each of the independent subduction zones in the Pacific Coast of Mexico. The seismic hazard assessment was determined using the total probability theorem according to Eq. (4).

$$F(A > a) = \int_A \int_M \int_R \int_T f_{A|M,R}(a) f_M(m|t) f_R(r) dm dr dt da \tag{4}$$

where, A is the peak ground acceleration, lognormally distributed; $F(A > a)$ is the probability of $A > a$; $f_{A|M}$, $R(a)$ is the probability distribution of the ground acceleration A, given the magnitude M and distance R,$f_M(m|t)$, is the magnitude distribution given the inter-occurrence time of earthquakes, $f_R(r)$ is the distance probability distribution between the epicenter and the site and $f_T(t)$ is the probability distribution of the time between earthquake occurrences.

The acceleration exceedance rate for the i seimic source was obtained as (Eq. (5))

$$\nu_i(a) = \sum_j P_{ij} P(A > a) \tag{5}$$

where ν_i is the acceleration exceedance rate for the i seimic source and P_{ij} is a weighting parameter to involve the size of each j element in the source i. Hence, the acceleration exceedance rate for all sources is

$$\nu(a) = \sum_{i=1}^{n} \nu_i(a) \tag{6}$$

The exceedance rate of the peak ground acceleration, a, was obtained by using Eq. (6). This gives the annual probability of exceedance of the acceleration a. Once determined the annual probability of exceedance curves (ν), four return periods ($Tr = 1/\nu$) are chosen for scaling the accelerograms. Table 1 summarizes the peak ground acceleration ($a = \text{PGA}$) obtained for the selected four earthquake return periods. All the seismic records used in the study for the seismic vulnerability assessment of the bridges were scaled to the values showed in Table 1. It must be mentioned that this interval of return periods have been extensively used in other sites of the world (Pitilakis *et al.* 2011).

4. Seismic excitation

A collection of 116 seismic records of subduction type and 43 seismic records of intraplate type earthquakes were selected for the demand assessment. In the first case, all the records selected belong to earthquakes with a minimum magnitude of 7.0, and in the second case to earthquakes with a minimum magnitude of 6.5. In both cases, the seismic stations are always situated in a range of 50 km to 150 km from the earthquake epicenter.

5. Seismic demands

The expected spectral pseudoacceleration and displacement demands on the bridges were determined as the average value of the spectral ordinates for each period of the response spectra obtained with the collection of the scaled seismic records. These demands were evaluated for two orthogonal directions that corresponded to seismic records acting in the longitudinal and transverse directions of the bridge, the analyses were carried considering the earthquakes acting independently in each direction. Fig. 4 shows the average pseudoacceleration response spectrum of the subduction earthquake records, for each of the four return periods (50, 235, 500 and 1000 years).

6. Seismic capacity

The bridges seismic capacity was estimated with a nonlinear static analysis that models the nonlinear behavior of the piers through the definition of plastic hinges at the top and at the bottom of each element. Plastic hinges are modeled as a discrete point hinge with plastic deformation occurring within the point hinge. This point was assumed to occur at 10% of the column height ends. The plastic hinges were modeled as coupled axial-force/biaxial-moment behavior. Fig. 5 shows the curve that describes de plastic hinge's behavior for the force-displacement or moment-rotation relationships. These curves define the yield value and the plastic deformation following the yield defined by the five points shown on it (*A*-*B*-*C*-*D*-*E*). The origin of the curve is always represented by point *A*; point *B* represents yielding and no plastic deformations occurs on the hinge up to this point, e.g. only deformation beyond point *B* will be exhibited by the hinge; the ultimate capacity for pushover analysis is determined by point *C*; point *D* represents the residual stress

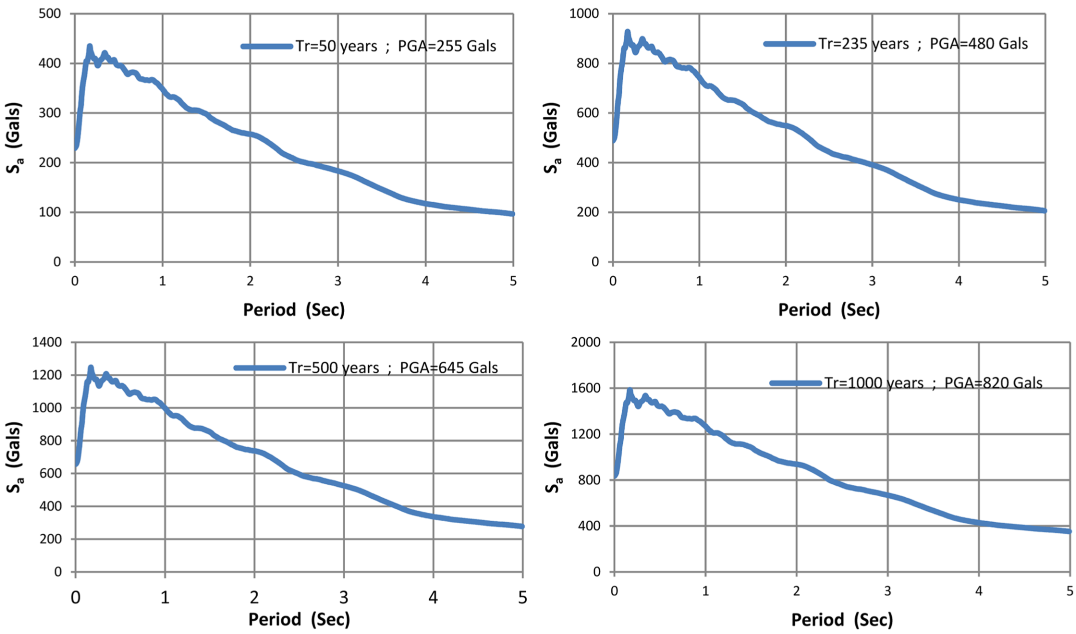

Fig. 4 Mean seismic demands for each of the subduction earthquake return periods

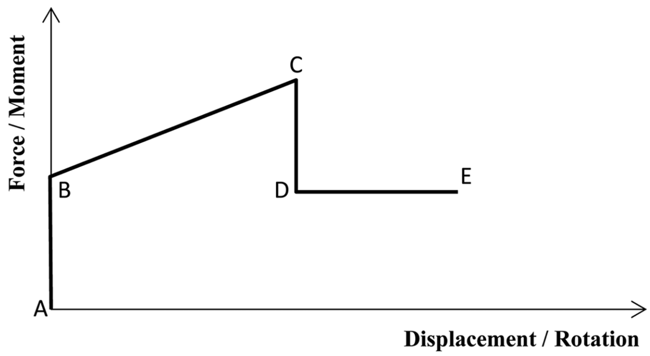

Fig. 5 Force plastic deformation curve

considered in the pushover analysis; and the total failure is given by point *E*. These points are used by the program to determine the pushover analysis.

The lateral load was applied on the geometrical center of each span of the deck. This process was achieved using the SAP2000 V14 program. The plastic hinges' properties were defined according to FEMA 356 in two ways: for the typical representative bridges the plastic hinges were designed directly by the program as it is stipulated in FEMA 356; for the existent bridges, the Chuta Bridge and the Feliciano Bridge, the plastic hinges were defined according to their moment-curvature relationships.

7. Vulnerability assesment

The estimation of the bridges' vulnerability was achieved using fragility curves defined as the conditional probability of attaining or exceeding a specified limit state. In this analysis, the *C*/*D* ratio was selected as the vulnerability parameter as shown in Eq. (7). The capacity *C* and demand *D* are continuous random variables that were modeled with a lognormal distribution. This means that the *C*/*D* ratio is log-normally distributed as well. Based on the limit state function, the fragility curve for a structural system with random variables of this type is given by a lognormal cumulative probability density function (Eq. (8)).

$$g(S_d) = \frac{C(S_d)}{D(S_d)} \tag{7}$$

$$F(S_d) = P\{[g(S_d) \leq 1.0] | S_d\} \tag{8}$$

where $C(S_d)$ and $D(S_d)$ represent the capacity and the demand for a given spectral displacement S_d, and $P\{[g(S_d) \leq 1|S_d]\}$ is the conditional probability of failure, defined by a lognormal cumulative probability density function as explained previously. To define a lognormal density function, Eq. (9), it is required to determine two parameters: the median and *a* the logarithmic standard deviation S_d and σ_{Sd}. Eq. (10) defines the parameter μ_{Sd} for a given S_d that corresponds to the intersection point of the capacity and the demand functions, and the parameter σ_{Sd} was considered to be 0.3 and 0.6, values commonly used in seismic vulnerability studies of bridges (Mander 1999, Dutta and Mander 1998, Nielson and DesRoches 2007)

$$f_{S_d} = \frac{1}{S_d \sigma_{S_{d\sqrt{2\pi}}}} e^{-\frac{1}{2\sigma_{S_d}^2}[ln(S_d)-\mu S_d]^2} \tag{9}$$

$$\mu_{S_d} = ln(S_d) - \frac{\sigma_{S_d}^2}{2} \tag{10}$$

Once the capacity of each of the bridges and the expected demands was evaluated, the probability of failure of the bridges in longitudinal and transverse directions was assessed. Figs. 6 and 7 show the fragility curves in the longitudinal direction when considering that the ground motions act only in the longitudinal direction of the selected group of typical bridges for returns periods of 50, 235, 500 and 1000 years, for the frame type (three columns) and one column pier configurations respectively. The first and second rows of the plots correspond to bridges with piers' heights of 6 and 10 m. In a similar manner, the first and second columns of the plots are for bridges with a span length of 20 and 40 m, respectively. Figs. 8 and 9 show the fragility curves of these bridges in the transverse direction, considering that the ground motions act only in the transverse direction of the bridge.

The results presented in Figs. 6 through 9 represent the probability of exceeding a particular limit state of damage linked to the return periods considered in the analysis. The limit states go from light structural damage on the bridge piers (50-year return period) to severe damage of the bridge (1000-year return period). In general, the probability of reaching a limit state decreased for longer

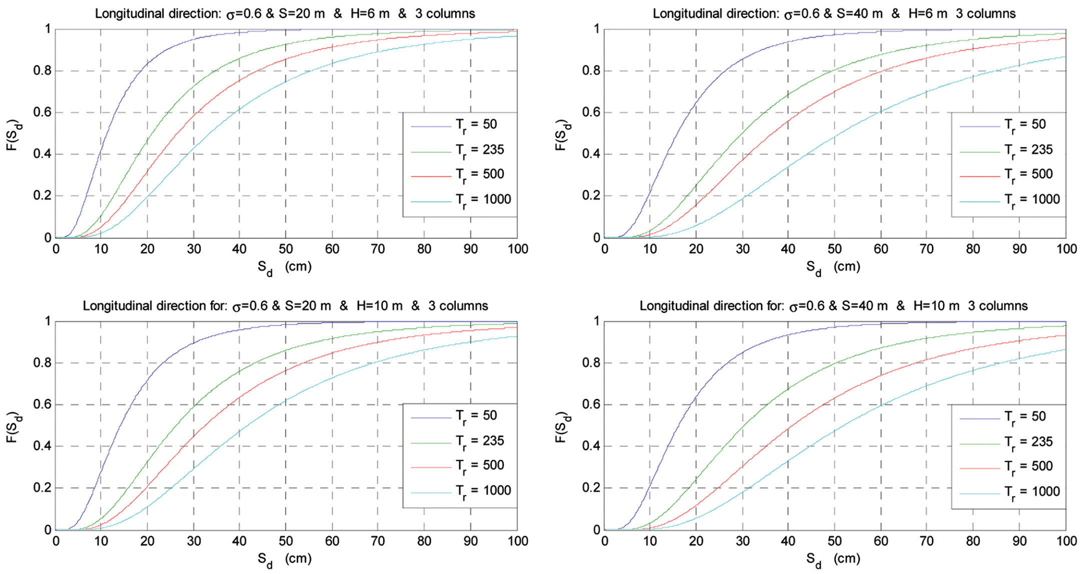

Fig. 6 Fragility curves in longitudinal direction of the three column pier bridges' model for $\sigma_{Sd} = 0.6$ and for different return periods

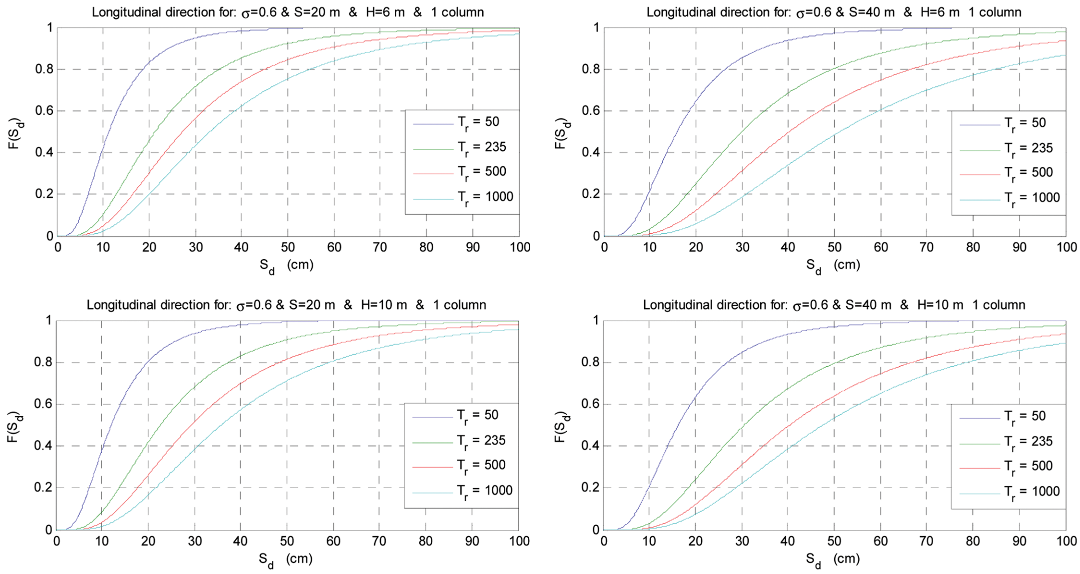

Fig. 7 Fragility curves in the longitudinal direction of the one column pier bridges' model for $\sigma_{Sd} = 0.6$ and for different return periods

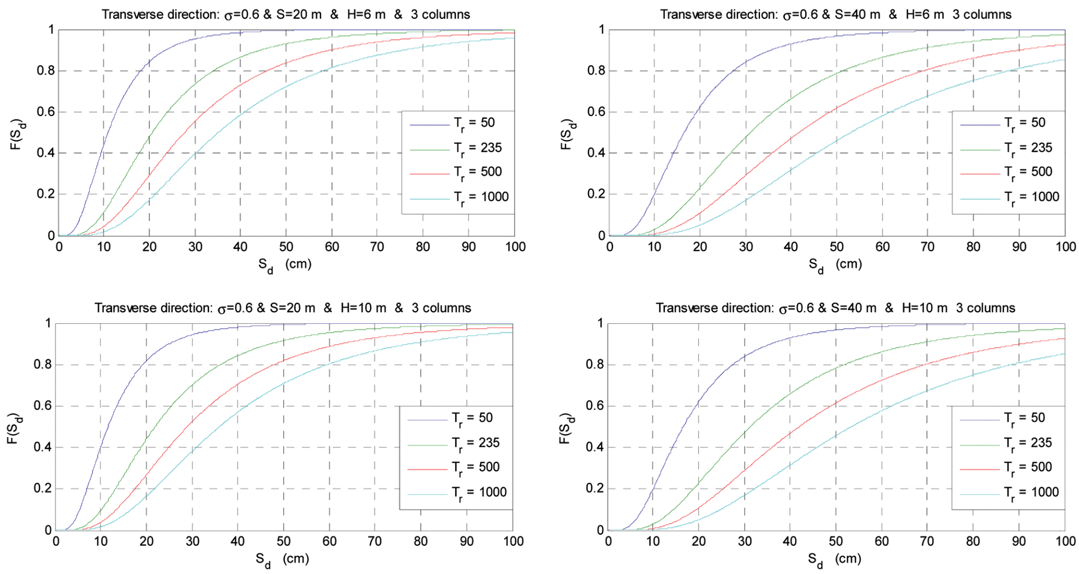

Fig. 8 Fragility curves in the transverse direction of the three column pier bridges' model for $\sigma_{Sd} = 0.6$ and for different return periods

return periods, as could be expected, the reductions are bigger for the 40 m span length. The fragility curves resulted to be sensitive to the bridge span length (20 or 40 m) and to the pier height (6 or 10 m) although the fragilities change when comparing the values considered for each variable. This is also the case for bridges where the pier height is the only geometric parameter that differs, particularly for shorter return periods. Results show similar trends for the transverse direction (Figs. 8 and 9).

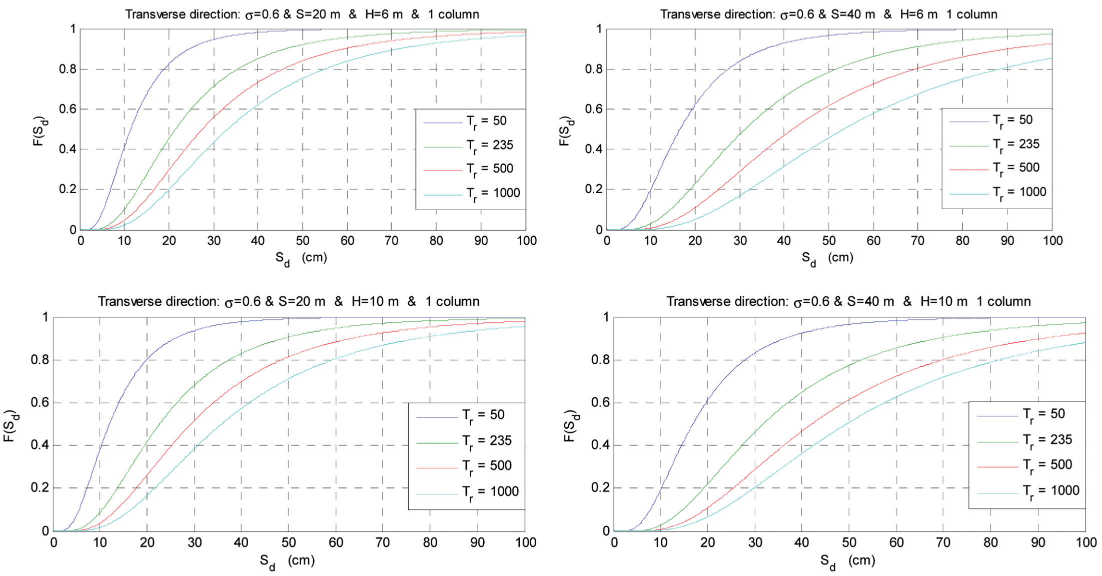

Fig. 9 Fragility curves in the transverse direction of the one column pier bridges' model for $\sigma_{Sd} = 0.6$ and for different return periods

To look at the applicability of the fragility curves obtained for typical bridge models to the existing ones, the fragility curves for the Chuta and the Feliciano bridges were determined. Figs. 10 and 11 show the fragility curves obtained for these two bridges in their longitudinal and transverse directions, respectively. In both of the figures, the first and second row present the fragility curves of the Chuta and Feliciano bridges, respectively. The plots in the first and second columns are the results obtained for two σ_{Sd} values (0.6 and 0.3, respectively).

When comparing the results of the Chuta Bridge versus bridge models with one-column pier substructures, and the Feliciano Bridge versus bridge models with frame type substructures, it is possible to study the applicability of the fragility curves presented in Figs. 6 to 8. The probability of exceeding a particular limit state in the existing bridges, Figs. 10 and 11, show that, on average, the fragility curves present similar tendencies to the ones previously discussed for the corresponding general model. The estimation of the probability of attaining a limit state for one of the real bridges using the fragility curves evaluated with the parametric analysis is more accurate when considering a standard deviation of 0.6. Further, it resulted that the fragility curves generated for the three columns frame-type substructure are applicable to the two columns frame-type substructure actual bridge.

In order to investigate the contribution of the parameters analyzed on the fragility curves, the probability of exceeding three of the limit states ($Tr = 50$ years, $Tr = 235$ years and $Tr = 1000$ years) for a specific displacement, used as an example, were determined. Table 2 shows these probability values for a drift of 0.03, obtained with the analysis of the ten bridge models.

As shown in table 2, the probability of exceeding the limit state related to $Tr = 50$ years is in the range of 62% to 96% as function of the span length, pier height, pier type and direction of analysis. These values are substantially reduced for the limit state of $Tr = 1000$ years. In this case, the probability values are in the range of 6% to 45%. These wide-open ranges confirm the remarkable influence of each of the parameters on the fragility estimates.

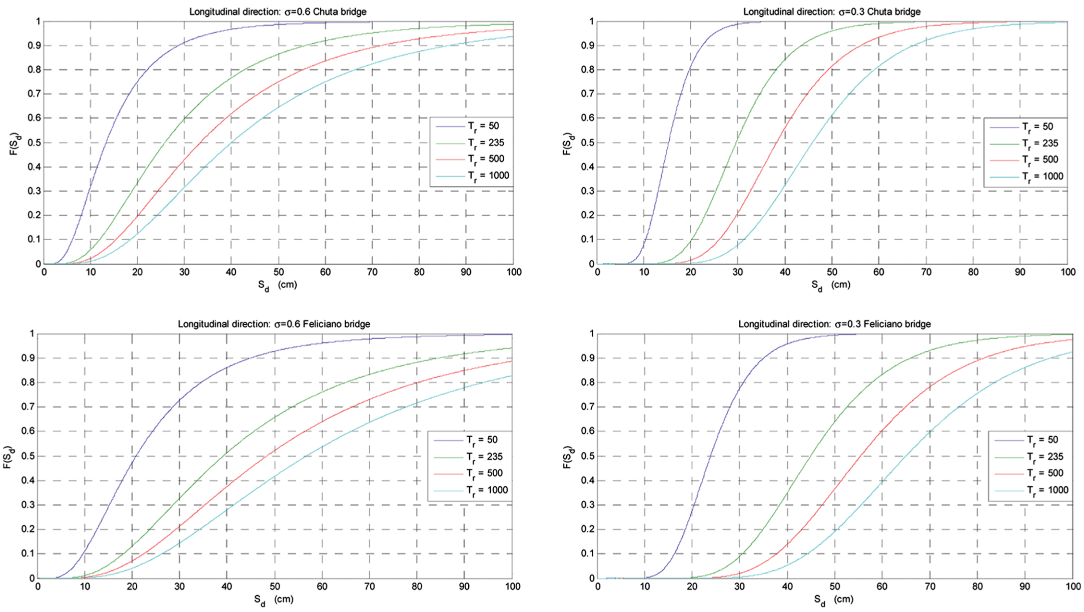

Fig. 10 Fragility curves in the longitudinal direction for the existent bridges for different return periods

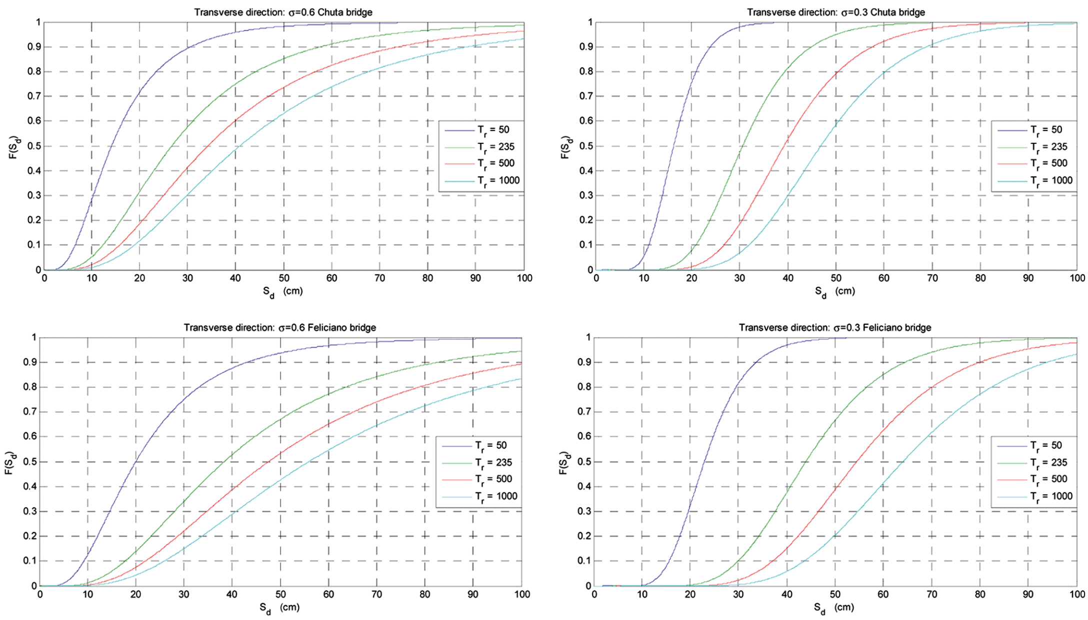

Fig. 11 Fragility curves in the transverse direction for the existent bridges for different return periods

Furthermore, the contribution of each parameter can be more clearly visualized if the piers' height, span length and pier type ratios are obtained as shown in Tables 3 to 5. Table 3 presents the probability ratio (model of 10 m piers' height/model of 6 m piers' height) of exceeding the three limit states. It is evident that the increase of this ratio to the increase of the bridge length, reflecting the importance on the fragility curves of the span length, changes. In the case of the 20-meter-long bridge models and the return period of 50 years, the probability ratio values were relatively small (1.22 maximum). However, these cases for a return period of 1000 years were noticeably increased, reaching a maximum value of 2.25, showing that the importance of the piers' height depends on the selected limit state. It must be emphasized that the probability of exceeding a limit state of the 10-meter piers model (for $Tr = 1000$ years), can be as much as 5.67 times the obtained value with the 6-meter-high model.

The influence of the span length in the probability of reaching a limit state decreases as this

Table 2 Probability of exceeding three limit states of behavior for a drift value of 0.03

Pier type	Direction of analysis	Bridge length (m)	Pier height (m)	Limit state probability		
				$Tr = 50$	$Tr = 235$	$Tr = 1000$
3 Columns	Longitudinal	20	6	0.83	0.47	0.20
			10	0.92	0.65	0.35
		40	6	0.64	0.25	0.06
			10	0.88	0.55	0.22
1 Column		20	6	0.83	0.45	0.20
			10	0.95	0.73	0.45
		40	6	0.65	0.26	0.06
			10	0.88	0.55	0.27
3 Columns	Transverse	20	6	0.84	0.49	0.18
			10	0.96	0.75	0.43
		40	6	0.62	0.23	0.06
			10	0.87	0.53	0.20
1 Column		20	6	0.82	0.46	0.20
			10	0.95	0.74	0.45
		40	6	0.62	0.23	0.05
			10	0.87	0.53	0.25

Table 3 Probability ratio of the two pier height models ($H = 10$ m/$H = 6$ m)

Piers type	Direction of analysis	Bridge length (m)	$Tr = 50$	$Tr = 235$	$Tr = 1000$
3 Columns	Longitudinal	20	1.14	1.48	1.93
		40	1.47	2.45	4.5
1 Column		20	1.19	1.74	2.53
		40	1.46	2.58	5.5
3 Columns	Transverse	20	1.18	1.67	2.92
		40	1.5	2.61	5.67
1 Column		20	1.22	1.74	2.53
		40	1.48	2.42	5.00

Table 4 Probability ratio of the two length models ($L = 20$ m/$L = 40$ m)

Piers type	Direction of analysis	Pier height (m)	$Tr = 50$	$Tr = 235$	$Tr = 1000$
3 Columns	Longitudinal	6	1.30	1.88	3.33
		10	1.05	1.18	1.59
1 Column		6	1.28	1.73	3.33
		10	1.08	1.33	1.67
3 Columns	Transverse	6	1.35	2.13	3.00
		10	1.10	1.42	2.15
1 Column		6	1.32	2.00	4.00
		10	1.09	1.40	1.80

Table 5 Probability ratio of the substructure type models (1 column/3 columns)

Direction of analysis	Bridge length	Pier height (m)	$Tr = 50$	$Tr = 235$	$Tr = 1000$
Longitudinal	20	6	1.00	0.96	1.00
	20	10	1.03	1.12	1.29
	40	6	1.02	1.04	1.00
	40	10	1.00	1.00	1.23
Transverse	20	6	0.98	0.94	1.11
	20	10	0.99	0.99	1.05
	40	6	1.00	1.00	0.83
	40	10	1.00	1.00	1.25

variable increases, as Table 4 shows. The tendency applies for both of the column heights considered, but larger columns have smaller ratios than the shorter piles. This result is understandable given the fact that taller piles should be more susceptible under seismic loads. Further, when the span length increases, the design requires a larger column cross section (increasing the piers' stiffness), which is reflected in its period changes that could led to different seismic demands. In all cases, the probability values of the 20-meter-long models are larger than those values of the 40-meter-long spans. The tendency described is also valid for the two type of substructures, and for the longitudinal and transverse directions.

From a practical point of view, the Tables 3 and 4 show that the probability of reaching a target displacement does not have a significant change when the span length or the pier height are varied, for the service limit state. On the other hand, when considering the collapse prevention limit state, special care must be taken in the evaluation of the seismic vulnerability as a function of these parameters. The later means that the service limit state conditions allow grouping a less number of bridge typologies as a function of their span length and piers height making attractive the use of simplified methodologies to evaluate the bridge seismic vulnerability for frequent earthquakes.

Table 5 presents the probability ratio (1 column model/3 columns model) of exceeding the three limit states for the two substructure types. Results show that, in all cases, the substructure type is irrelevant when the limit state of the $Tr = 50$ years is considered. On the other hand, the type of substructure is a significant parameter if the bridge height is 10 meters and it is less important when the 6-meter-high bridge is analyzed. The substructure type was the variable of the parameters analyzed with minor influence on the fragility curves.

Therefore, it can be said that the bridge models analyzed could be used as representative of bridges in Mexico with span length in the range of 20 to 40 m and piers' heights of 6 to 10 m, with substructure formed by RC piers of one, two or three columns (frame type substructures). The results obtained from this work show that it is possible to use the fragility curves developed here to assess the probability of reaching different limit states as a function of the earthquake displacement demand to determine the seismic vulnerability for a very common type of bridges in Mexico.

8. Conclusions

In this work, the influence of some parameters on the probability of exceeding a particular limit state of damage for a group of ten bridge models with geometries similar to the most common bridges built in Mexico was evaluated. The fragility curves for two existing bridges were also determined. All of the selected bridges are located on the Pacific Coast of Mexico, the most vulnerable seismic zone of the country. The bridge capacities were determined by conducting nonlinear static analyses. The seismic demand was estimated based on a seismic hazard assessment and by using 116 seismic records for an earthquake return periods of 50, 235, 500 and 1000 years. The capacity and the demand were considered as continuous random variables characterized with a lognormal probability density function, as a result the fragility curves are defined with a lognormal cumulative density function. The similar trends of behavior between the existing bridges studied and the bridge models analyzed, allow using the fragility curves obtained to assess the seismic vulnerability on other existing bridges with similar characteristics of the bridges studied.

Results show the importance of the piers' height, which depends on the selected limit state. The probability of exceeding the most severe limit state studied ($Tr = 1000$ years) in the 6-meter-height piers' model can be as much as 4.5 times the obtained value with the 10-meter-high model.

The influence of the span length in the probability of reaching a limit state decreases as this variable increases. The tendency applies for both of the column heights considered, but larger columns have smaller ratios than the shorter piers. In all cases, the probability values of the 20-meter-long models are larger than those values of the 40-meter-long spans. The tendency described is also valid for substructures conformed with three (frame type substructure) and one pier, and for the seismic response of bridges in the longitudinal and transverse direction.

As it is well known, one of the variables that mostly affect the seismic vulnerability of a bridge is substructure type (one column or frame types); in spite of this fact, the results showed that this variable have a bigger or smaller impact as function of two parameters: the expected PGA and the limit state of behavior analyzed. For the cases considered, it happened to be that only slightly influence of all the parameters considered was presented for the service limit state ($Tr = 50$ years) and the smallest expected PGA. It means that there were not important differences among the probabilities of reaching this limit state.

On the other hand, the influence of all variables can be quite significant if other limit states of behavior are studied. Changes in the substructure type, span length and bridge height affect importantly the probability of reaching a specific displacement demand, as shown in Tables 3 and 4.

The substructure type was the variable of the parameters analyzed, with minor influence on the fragility curves.

In spite of the contribution that traditional variables (height and substructure type) had to the bridge seismic response, bridge length was also found to be one of the parameters that most contributed to the seismic vulnerability of these RC medium length bridges.

References

AASHTO (2002), *Standard specification for highway bridges*, 17th edition, American Association of State Highway and Transportation Officials, Washington, D.C.

Abrahamson, N.A. and Silva, W.J. (1997), "Empirical response spectral attenuation relations for shallow crustal earthquakes", *Seismol. Res. Lett*., **68**(1), 94-127.

Ali, M.R. and Okabayashi, T. (2011), "System identification of highway bridges from ambient vibration using subspace stochastic realization theories", *Earthq. Struct*., **2**(2), 189-206.

ATC-40 (1996), *Seismic evaluation and retrofit of concrete buildings*, Redwood City, California: Applied Technology Council, ATC-40.

ATC/BSSC (1997), *NEHRP Guidelines for the seismic rehabilitation of buildings*, FEMA 273 Report (Guidelines) and FEMA 274 Report (Commentary), prepared by the Applied Technology Council for the Building Seismic Safety Council, published by the Federal Emergency Management Agency, Washington, D.C.

Banerjee, S. and Shinozuka, M. (2007), *Nonlinear static procedure for seismic vulnerability assessment of bridges*, At. Irvine, CA: Department of Civil and Environmental Engineering, University of California.

Dutta, A. and Mander, J. (1998), *Seismic fragility analysis of highway bridges*, In: INCEDE-MCEER workshop on earthquake engineering frontiers in transportation systems, Tokyo.

DiPasquale, E. and Cakmak, A.S. (1990), "Seismic damage assessment using linear models", *Soil Dyn. Earthq. Eng*., **9**(4), 194-197.

FEMA 356 (2000), *NEHRP Guidelines for the seismic rehabilitation of buildings*, Federal Emergency Management Agency, Washington, D.C.

Fridley, K.J. and Ma, Z. (2007), *Reliability-based design of seismic retrofit for bridges*, Olympia, Washington, Washington State Department of Transportation, Technical report W-R 664.1.

García, D., Singh, S.K., Herraiz, M., Ordaz, M. and Pacheco, J.F. (2005), "Inslab earthquakes of central Mexico: peak ground-motion parameters and response spectra", *B. Seismol. Soc. Am*., **95**(6), 2272–2282.

Gómez Soberón, C., Oller, S. and Barbat, A.H. (2002), "Assessment of the seismic vulnerability of bridges using simple models", *Monogr. Seism. Eng*., Universidad Politécnica de Cataluña.

Hwang, H., Jernigan, J.B. and Lin, Y.W. (1998), *Evaluation of seismic damage to bridges and highway systems in Shelby county, Tennessee*, Memphis: Technical Report, Center for Earthquake Research and Information, University of Memphis.

Hwang, H., Jernigan, J.B. and Lin, Y.W. (2000), "Evaluation of seismic damage to Memphis bridges and highway systems", *J. Bridge Eng*., **5**(4), 322-330.

Jara, J.M., Madrigal, E., Jara, M. and Olmos, B.A. (2011), "Seismic source effects on the fragility curves of an irregular isolated bridge", *Earthq. Eng. Struct. D*.

Jara, J.M. and Rosenblueth, E. (1988), "Probability distribution of times between characteristic subduction earthquakes", *Earthq. Spectra*, **4**(3), 499-529.

Karim, K.R. and Yamazaki, F. (2003), "A simplified method of constructing fragility curves for highway bridges", *Earthq. Eng. Struct. D*., **32**(32), 1603-1626.

Kasperski, A., Matarazzo, J.B., Santos, J.A., Wang, G. and Yiu, C.S.C. (2006), "Seismic vulnerability assessments of bridges in areas of low to moderate seismic activity", *Fifth national seismic conference on bridges & highways*, San Francisco, CA.

Kim, S.H. and Shinozuka, M. (2004), "Development of fragility curves of bridges retrofitted by column jacketing", *Probabilist. Eng. Mech*., **19**(1-2), 105-112.

Mackie, K. and Stojadinovic, B. (2006), "Seismic vulnerability of typical multiple-span California highway bridges", *Fifth national seismic conference on bridges & highways*, 18-20 September, San

Mander, J.B. (1999), "Fragility curve development for assessing the seismic vulnerability of highway bridges", *MCEER Highway Project/FHWA*, National Institute of Building Sciences (NIBS).

Moses, F. (1999), *Bridge reliability concepts and methods*, Bridge Safety and Reliability, Chapter 1, 1-22.

Moustafa, A. and Mahadevan, S. (2011), "Reliability analysis of uncertain structures using earthquake response Spectra", *Earthq. Struct*., **2**(3), 279-295.

Nielson, B.G. (2005), Analytical fragility curves for highway bridges in moderate seismic zones, Ph.D. Dissertation, School of Civil and Environmental Engineering, Georgia Institute of Technology.

Nielson, B.G. and DesRoches, R. (2007), "Seismic fragility methodology for highway bridges using a component level approach", *Earthq. Eng. Struct. D.*, **36**(6823-6839), 823-839.

Padgett, J. (2005), "Retrofitted bridge fragility curves for assessing the consequences of an earthquake event", *Mid-America Earthquake Center, Student Leadership Council Online Magazine V*, University of Illinois at Urbana-Champaign.

Pagnini, L.C., Vicente, R., Lagormarsino, S. and Varum, H. (2011), "A mechanical model for the seismic vulnerability assessment of old masonry buildings", *Earthq. Struct*., **2**(1), 25-42.

Panza, G.F., Romanelli, F. and Vaccari, F. (2001), *Effects on bridge seismic response of asynchronous motion at the base of the bridge piers*, International Center of Theoretical Physics (ICTP), Report 5/1,2,3F, Trieste, Italy.

Pekcan, G. (1998), *Design of seismic energy dissipation systems for concrete and steel structures*, Ph.D. Dissertation, University at Buffalo, State University of New York, Buffalo, New York.

Pitilakis, K.D., Anastasiadis, A.I., Kakderi, K.G., Manakou, M.V., Manou, D.K., Alexoudi, M.N., Fotopoulou, S.D., Argyroudis, S.A. and Senetakis, K.G. (2011), "Development of comprehensive earthquake loss scenarios for a Greek and a Turkish city: seismic hazard, geotechnical and lifeline aspects", *Earthq. Struct*., **2**(3), 207-232.

Rosenblueth, E. and Ordaz, M. (1989), "Maximum earthquake magnitude at fault", *J. Eng. Mech*., **116**(1), 204-216.

Rosenblueth, E., Mario Ordaz, F.J., Sesma, S. and Singh, S.K. (1989), "Design spectra for Mexico's federal district", *Earthq. Spectra*, **5**(1), 273-291.

Shinozuka, M., Banerjee, S. and Kim, S.H. (2007), *Statistical and mechanistic fragility analysis of concrete bridges*, New York: MCEER, University of Buffalo. Technical Report MCEER-07-0015, 171.

Sánchez, A.R. and Jara, J.M. (2001), "Attenuation laws for the Michoacan State", (in Spanish), *Revista de la Coordinación de Investigación Científica*, UMSNH, **27**, 91-106.

Shinozuka, M., Banerjee, S. and Kim, S.H. (2007), *Statistical and mechanistic fragility analysis of concrete bridges*, New York: MCEER, University of Buffalo. Technical Report MCEER-07-0015, 171.

Yi, J.H., Dookie, K. and Feng, M.Q. (2009), "Periodic seismic performance evaluation of highway bridges using structural health monitoring system", *Struct. Eng. Mech*., **31**(5), 527-544.

SA